# Beamspace MIMO for High-Dimensional Multiuser Communication at Millimeter-Wave Frequencies

Akbar Sayeed and John Brady
Electrical and Computer Engineering
University of Wisconsin - Madison
Madison, WI, USA

***Abstract*—Millimeter-wave (mm-wave) systems operating from 30-300GHz provide a unique opportunity for meeting the exploding capacity demands on wireless networks. In addition to orders-of-magnitude larger bandwidths, the small wavelengths at mm-wave enable high-dimensional multiple-input multiple-output (MIMO) operation. However, fully exploiting the advantages of mm-wave requires prohibitively high transceiver complexity when using conventional MIMO techniques. In this paper we propose and analyze the sum capacity of several linear, reduced-complexity multiuser MIMO (MU-MIMO) precoders that exploit the concept of beamspace MIMO (B-MIMO) communication – multiplexing data onto orthogonal spatial beams that serve as approximate channel eigenfunctions. Due to quasi-optical propagation at mm-wave, MIMO channels are expected to be low-rank and the low channel rank is manifested in the sparsity of the beamspace channel matrix. This enables near-optimal rank and complexity reduction via the concept of multi-beam selection. We present numerical capacity results that demonstrate the reduced-complexity B-MIMO precoders are able to closely approximate the performance of their full-dimensional counterparts with complexity that tracks the number of mobile stations (MSs). In mm-wave systems, where the number of MSs is expected to be much lower than the system dimension, this enables a considerable reduction in the digital signal processing complexity and in systems equipped with analog beamforming front-ends the hardware complexity is also reduced. Thus, the proposed reduced-complexity multiuser precoders provide a near-optimal route for achieving multi-Gigabit/s sum rates in mm-wave MU-MIMO networks with the lowest transceiver complexity.**

***Index Terms*—millimeter-wave wireless, Gigabit wireless, high-dimensional MIMO, massive MIMO, beamforming, multiuser precoders**

## I. Introduction

The capacity demands on wireless networks are growing exponentially with the proliferation of data intensive wireless devices, such as smart phones and tablets. In current wireless networks operating below 5 GHz, two main approaches are being pursued for addressing this challenge: small cells to increase spatial re-use of spectrum [1], [2], and multi-antenna multiple-input multiple-output (MIMO) technology for managing interference and increasing spectral efficiency [3], [4]. Emerging millimeter-wave (mm-wave) systems, operating from 30-300GHz, offer a complementary, synergistic opportunity due to the orders-of-magnitude larger available bandwidth [5], as well as high-dimensional MIMO operation due to the small wavelengths [6], [7]. The large number of MIMO degrees of freedom can be exploited for a number of critical capabilities, including [5]–[8]: higher antenna/beamforming gain for enhanced power efficiency; higher spatial multiplexing gain for enhanced spectral efficiency; and highly directional communication with narrow beams for reduced interference and enhanced security.

The extremely *narrow beamwidths* at mm-wave (Fig. 1(a)) offer a powerful and complementary alternative to small cells through *dense spatial multiplexing*: reuse of spectral resources across distinct beams [6], [7]. The spatial multiplexing gain, coupled with the larger bandwidths, promise unprecedented gains in network throughput and spectral efficiency even over larger spatial scales due to the large *antenna directivity gains* (Fig. 1(b)). Fig. 1(c) shows idealized spectral efficiency upper bounds for downlink communication from an access point (AP) with a 6"x6" antenna. While at 3GHz a maximum of 9 mobile stations (MSs) can be spatially multiplexed, at 80GHz orders-of-magnitude improvements are possible in signal-to-noise ratio (SNR) due to antenna gain, and in spectral efficiency due to spatial multiplexing gain. Indeed, 100-10,000 Gigabits/s (Gbps) aggregate rates (over 100-300 MSs) seem attainable with the 1-10GHz of available mm-wave bandwidth.

However, unleashing the full potential of the mm-wave spectrum makes agile electronic beamforming, and associated MIMO techniques, a critical functionality. This, in turn, presents significant challenges in terms of *transceiver complexity* due to the *high dimension* ($n$) of the spatial signal space [5]–[7]. Approaches to reducing complexity (e.g., antenna selection [9], [10] and widely spaced antennas [11]–[14]) are sub-optimal and suffer from severe performance degradation [6], [7]. Due to the predominance of line-of-sight (LoS) and sparse multipath propagation at mm-wave frequencies [5], [15], MIMO channels are expected to be low-rank: communication occurs in a low-dimensional subspace of the high-dimensional spatial signal space.

In this paper, we propose transceiver architectures that exploit the concept of beamspace MIMO (B-MIMO) communication – multiplexing data onto orthogonal spatial beams – for near-optimal performance at mm-wave frequencies with transceiver complexity that tracks the dimension of the communication subspace [6], [7]. A key advantage of B-MIMO is that orthogonal beams serve as approximate channel

This work is partly supported by the NSF under grants ECCS-1052628 and ECCS-1247583, and the Wisconsin Alumni Research Foundation.

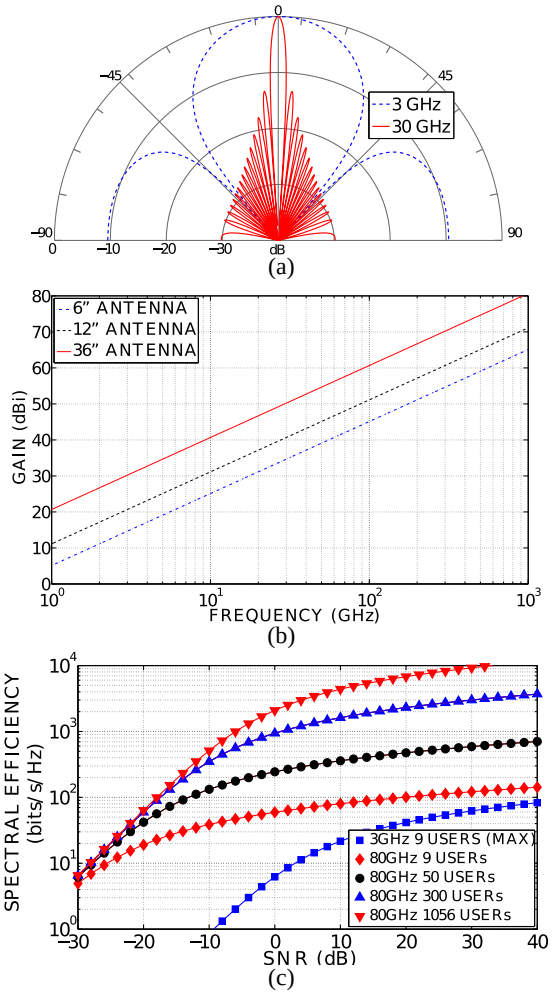


Fig. 1: (a) Antenna beampatterns for a 6" antenna at 3GHz vs. 30GHz. (b) Antenna gain vs. frequency. (c) Potential multiuser spectral efficiency gains due to spatial multiplexing at 80GHz vs. 3GHz with a 6" $\times$ 6" antenna.

eigenfunctions [6], [7], [16]. Thus, the low channel rank is manifested in the sparsity of the beamspace channel matrix. This naturally leads to *beam selection* for near-optimum dimensionality reduction, which can be exploited for dramatic reduction in transceiver complexity on two fronts. In conventional massive MIMO systems [8], B-MIMO techniques can be used to reduce the digital signal processing (DSP) complexity. In systems that use analog beamforming, e.g via a discrete lens array fed by an array of beamspace antennas as in Continuous Aperture Phased MIMO (CAP-MIMO) [6], [7], [17] or via phase shifting networks in conventional antenna arrays [5], [18], a significant reduction in hardware complexity can be achieved as well.

We develop and compare the capacity of three linear, reduced-complexity B-MIMO precoders for multiuser MIMO (MU-MIMO) links: the matched-filter (MF), zero-forcing (ZF) and Wiener filter (WF) precoders. We demonstrate that the performance of the reduced-complexity B-MIMO precoders is nearly identical to that of their full-dimensional counterparts with complexity that tracks the number of MSs. At mm-wave the number of MSs is expected to be orders-of-magnitude lower than the system dimension. Thus, the combination of reduced-complexity B-MIMO precoding and systems equipped with analog beamforming front-ends provides a near-optimal route for attaining multi-Gbps speeds in mm-wave MU-MIMO networks with the lowest transceiver complexity.

## II. System Model

We focus on an access point (AP) with a multi-antenna array communicating with $K$ single-antenna mobile MSs. We examine the more challenging scenario of downlink communication - the uplink problem is well-studied [19] and can be formulated easily along the lines discussed here. Let the AP be equipped with an $n$-dimensional antenna which we consider to be a critically-sampled uniform linear array (ULA) for simplicity. We note that this model also captures the performance of APs equipped with continuous aperture antennas that perform analog beamforming [6], [7]. The received signal at the $i^{\text{th}}$ MS is given by

$$r_i = \mathbf{h}_i^H \mathbf{x} + w_i$$

where $\mathbf{x}$ is the $n$-dimensional transmitted signal, $\mathbf{h}_i$ is the $n$-dimensional channel vector, and $w_i \sim \mathcal{CN}(0, \sigma^2)$ is additive white Gaussian noise (AWGN). Stacking the signals for all MSs in a $K$ dimensional vector $\mathbf{r} = [r_1, \cdots, r_K]^T$ we get the antenna domain system equation

$$\mathbf{r} = \mathbf{H}^H \mathbf{x} + \mathbf{w} \ , \ \mathbf{H} = [\mathbf{h}_1, \cdots, \mathbf{h}_K] \tag{1}$$

where $\mathbf{H}$ is the $n \times K$ channel matrix that characterizes the system. Our focus is on the design of the linear precoding matrix $\mathbf{G}$ for the transmitted signal, $\mathbf{x} = \mathbf{G}\mathbf{s} = \sum_{i=1}^{K} \mathbf{g}_i s_i$, where $\mathbf{s}$ is the $K$ dimensional vector of independent symbols for different MSs. The overall system equation becomes

$$\mathbf{r} = \mathbf{H}^H \mathbf{G}\mathbf{s} + \mathbf{w} \ , \ E[\|\mathbf{x}\|^2] = \text{tr}(\mathbf{G}\mathbf{\Lambda}_s\mathbf{G}^H) \leq \rho \tag{2}$$

where the second equality represents the constraint on total transmit power, $\rho$, and $\mathbf{\Lambda}_s = E[\mathbf{s}\mathbf{s}^H]$ denotes the diagonal correlation matrix of $\mathbf{s}$.

### A. Channel Model

The channel matrix $\mathbf{H}$ governs the performance of the MU-MIMO link. For a critically-sampled, $n$-dimensional ULA, the channel can be accurately modeled via the array steering vector

$$\mathbf{a}_n(\theta) = [e^{-j2\pi\theta i}]_{i \in \mathcal{I}(n)} \ , \ \theta = 0.5 \sin(\phi) \tag{3}$$

where $\mathcal{I}(n) = \{i - (n-1)/2 : i = 0, 1, \cdots n-1\}$ is a symmetric set of indices centered around 0. The steering vector $\mathbf{a}_n(\theta)$ represents a discrete, complex spatial sinusoid whose spatial frequency $\theta \in [-0.5, 0.5]$ corresponds to a point source in the direction $\phi \in [-\pi/2, \pi/2]$ [6], [7], [16].[1]

Due to the highly directional and quasi-optical nature of propagation at mm-wave frequencies, line of sight (LoS) propagation is the predominant mode of propagation, with possibly a sparse set of single-bounce multipath components

[1]For a uniform planar array, the 2D steering vector is given by the Kronecker product of the steering vectors for the azimuth and elevation angles: $\mathbf{a}_n(\theta_a, \theta_e) = \mathbf{a}_{n_x}(\theta_a) \otimes \mathbf{a}_{n_y}(\theta_e)$ [6].

[15]. We assume that LoS paths exist for all MSs. Let $\theta_{k,0}$, $k = 1, \cdots, K$, denote the LoS directions (spatial frequencies) for the $K$ MSs. Then the LoS channel for the $k^{\text{th}}$ MS is $\mathbf{h}_k = \beta_{k,0}\mathbf{a}_n(\theta_{k,0})$, where $\beta_{k,0}$ is the complex path loss. In general, for sparse multipath channels

$$\mathbf{h}_k = \beta_{k,0}\mathbf{a}_n(\theta_{k,0}) + \sum_{i=1}^{N_p} \beta_{k,i}\mathbf{a}_n(\theta_{k,i}) \tag{4}$$

where $\{\theta_{k,i}\}$ denote the path angles and $\{\beta_{k,i}\}$ represent the complex path losses associated with the different paths for the $k^{\text{th}}$ MS. The amplitudes $|\beta_{k,i}|$ for multipath components are typically 5 to 10dB weaker than the LoS component $|\beta_{k,0}|$ [15]. In this paper, we focus on purely LoS channels with $\theta_{k,0} = \theta_k$, $|\beta_{k,0}| = 1$, and $\beta_{k,i} = 0$ for $i \neq 0$ for all MSs.

### *B. Beamspace System Model*

The beamspace MIMO system representation is obtained from (1) via fixed beamforming at the transmitter. The columns of the beamforming matrix, $\mathbf{U}_o$, are steering vectors corresponding to $n$ fixed spatial frequencies/angles with uniform spacing $\Delta\theta_o = \frac{1}{n}$ [6], [7], [16]:

$$\mathbf{U}_o = \frac{1}{\sqrt{n}}\left[\mathbf{a}_n\left(i\Delta\theta_o\right)\right]_{i\in\mathcal{I}(n)} \ , \ \Delta\theta_o = \frac{1}{n} = \frac{\lambda}{2L} \ , \tag{5}$$

which represent $n$ orthogonal beams that cover the entire spatial horizon ($-\pi/2 \leq \phi \leq \pi/2$), and form a basis for the $n$-dimensional spatial signal space. In fact, $\mathbf{U}_o$ is a unitary discrete Fourier transform (DFT) matrix: $\mathbf{U}_o^H\mathbf{U}_o = \mathbf{U}_o\mathbf{U}_o^H = \mathbf{I}$.

The beamspace system representation is obtained by choosing $\mathbf{G} = \mathbf{U}_o\mathbf{G}_b$ in (2)

$$\mathbf{r} = \mathbf{H}_b^H\mathbf{G}_b\mathbf{s}_b + \mathbf{w} \quad , \quad \mathbf{H}_b = \mathbf{U}_o^H\mathbf{H} = [\mathbf{h}_{b,1}, \cdots, \mathbf{h}_{b,K}] \tag{6}$$

where $\mathbf{s}_b = \mathbf{s}$ represents the beamspace symbol vector and $\mathbf{G}_b$ is the beamspace precoder. $\mathbf{x}_b = \mathbf{G}_b\mathbf{s}_b$ represents the precoded beamspace transmit signal vector (e.g. the signals on the feed antennas in CAP-MIMO). Since $\mathbf{U}_o$ is a unitary matrix, the beamspace channel matrix $\mathbf{H}_b$ is a completely equivalent representation of $\mathbf{H}$.

### *C. Beam Selection*

The most important property of $\mathbf{H}_b$ is that it has a sparse structure representing the directions of the different MSs, as illustrated in Fig. 2(a) for LoS links. The $k^{\text{th}}$ column $\mathbf{h}_{b,k} = \mathbf{U}_o^H\mathbf{h}_k$ (the rows in Fig. 2(a)) is the beamspace representation of the $k^{\text{th}}$ MS channel and has a few dominant entries near the true LoS direction $\theta_k$ of the MS. This sparse nature of the beamspace channel is exploited for designing reduced-complexity beamspace precoders that deliver near-optimal performance through the concept of beam selection.

We define the following sets of beam indices – *sparsity masks* – that represent the dominant beams that are selected for transmission at the AP (see Fig. 2(b)):

$$\begin{aligned}\mathcal{M}_k &= \left\{i \in \mathcal{I}(n) : |h_{b,k}(i)|^2 \geq \gamma_k \max_i |h_{b,k}(i)|^2\right\} \\ \mathcal{M} &= \bigcup_{k=1,\cdots,K} \mathcal{M}_k\end{aligned} \tag{7}$$

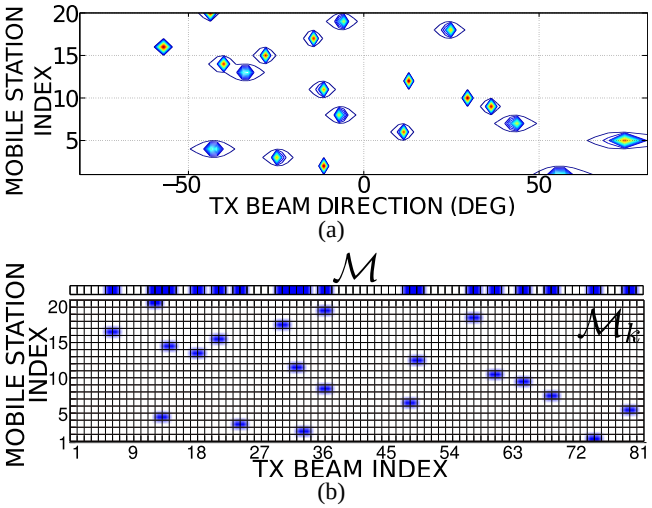


Fig. 2: (a) Contour plot of $|\mathbf{H}_b^H|^2$ for a ULA with $n = 81$, representing the *beamspace channel vectors* (rows) for 20 MSs randomly distributed between $\pm 90^o$ (b) Illustration of beamspace channel sparsity masks $\mathcal{M}_k$ and $\mathcal{M}$ for the $\mathbf{H}_b$ in (a).

where $\mathcal{M}_k$ is the sparsity mask for the $k^{\text{th}}$ MS, determined by the threshold $\gamma_k \in (0, 1)$. This beam selection is equivalent to selecting a subset of $p = |\mathcal{M}|$ rows of $\mathbf{H}_b$ resulting in the following low-dimensional system equation

$$\mathbf{r} = \tilde{\mathbf{H}}_b^H\tilde{\mathbf{G}}_b\mathbf{s}_b + \mathbf{w} \ , \ \tilde{\mathbf{H}}_b = [\mathbf{H}_b(\ell, :)]_{\ell\in\mathcal{M}} \ . \tag{8}$$

where $\tilde{\mathbf{H}}_b$ is the $p \times K$ beamspace channel matrix corresponding to the selected beams and $\tilde{\mathbf{G}}_b$ is the corresponding $p \times K$ precoder matrix, where $p \leq n$

For a given $\mathbf{H}$, the total multiuser channel power is defined as $\sigma_c^2 = \text{tr}(\mathbf{H}\mathbf{H}^H) = \text{tr}(\mathbf{H}_b\mathbf{H}_b^H)$, which under the simple LoS model is $\sigma_c^2 = n\sum_{k=1}^K |\beta_{k,0}|^2 = nK$. The beam selection thresholds $\{\gamma_k\}$ can be selected so that the $k^{\text{th}}$ column of $\tilde{\mathbf{H}}_b$ captures a significant fraction $\eta_k$ of the power of $\mathbf{h}_{b,k}$ (e.g $\eta_k \geq 0.9$). This, in turn, implies that the fraction $\eta$ of the channel power captured by $\tilde{\mathbf{H}}_b$ is at least $\min_{k=1,\ldots,K}\eta_k$.

Conversely, the sparsity masks $\mathcal{M}_k$ can be chosen to select the $m$ dominant (strongest) beams for each MS. This implicitly defines the $\{\gamma_k\}$ as the ratio between the power of strongest and $m^{\text{th}}$ strongest beams for each user. For the simple LoS channel model this corresponds to selecting the $m$ orthogonal beams closest to the true LoS direction of the MS $\theta_k$. In this paper we use a 2-beam mask for complexity reduction (see Fig. 2(b)). From the analysis in the Appendix, the expected value of $\eta$ for the 2-beam mask can be lower bounded as

$$E[\eta] \geq \frac{2}{n}\int_0^{\frac{\Delta\theta_o}{2}} f_n^2(\delta) + f_n^2(\delta - \Delta\theta_o)d\delta \tag{9}$$

where $f_n(\theta)$ is the Dirichlet sinc function.

## III. Multiuser Beamspace MIMO Precoders

There are three main types of linear MU-MIMO precoders: the matched filter (MF), zero-forcing (ZF), and Wiener filter (WF). For the full-dimensional antenna domain system (2), the

three precoders are given by [20]–[22]

$$\mathbf{G} = \alpha\mathbf{F} = \alpha[\mathbf{f}_1, \mathbf{f}_2, \cdots, \mathbf{f}_K] \ , \ \alpha = \sqrt{\frac{\rho}{\mathrm{tr}(\mathbf{F}\mathbf{\Lambda}_s\mathbf{F}^H)}} \quad (10)$$

$$\mathbf{F}_{MF} = \mathbf{H} \ , \ \mathbf{F}_{ZF} = \mathbf{H}(\mathbf{H}^H\mathbf{H})^{-1} \quad (11)$$

$$\mathbf{F}_{WF} = (\mathbf{H}\mathbf{H}^H + \zeta\mathbf{I})^{-1}\mathbf{H} \ , \ \zeta = \frac{\mathrm{tr}(\mathbf{\Sigma}_w)}{\rho} = \frac{\sigma^2 K}{\rho} \quad (12)$$

where the precoder matrix $\mathbf{G}$ is an $n \times K$ matrix. In beamspace, the equivalent full-dimensional precoder $\mathbf{G}_b$ can be obtained via the above equations by replacing $\mathbf{H}$ with $\mathbf{H}_b$. Similarly, the reduced-complexity B-MIMO precoder matrix $\tilde{\mathbf{G}}_b$ ($p \times K$) is obtained via (10)-(12) by replacing $\mathbf{H}$ with $\tilde{\mathbf{H}}_b$. As we demonstrate in the numerical results section, the reduced-complexity B-MIMO precoder can deliver the performance of the full-dimensional precoder with complexity that tracks the number of MSs $K$. The full dimensional precoders require $\mathcal{O}(n)$ MIMO processing for determining the $n \times K$ $\mathbf{G}$ as evident from (10)-(12). However, $\mathcal{O}(p)$ MIMO processing is needed for the low-dimensional B-MIMO system determined by the $p \times K$ $\tilde{\mathbf{H}}_b$. With an analog beamforming front-end, as in CAP-MIMO [6], [7], this also reduces the transceiver hardware complexity (the number of RF chains, including mixers, D/A or A/D converters, and power amplifiers) from $\mathcal{O}(n)$ to $\mathcal{O}(p)$.

## IV. Performance and Numerical Results

In this section, we assess the sum capacity of the B-MIMO precoders. Let $\rho$ denote the total transmit power, which equals the total transmit SNR for $\sigma^2 = 1$. We use the following idealistic upper bound for the sum capacity (spectral efficiency)

$$C_{ub}(\rho, K, n) = K \log_2\left(1 + \rho\frac{n}{K}\right) \text{ bits/s/Hz} \quad (13)$$

which corresponds to $K$ MSs with orthogonal channels (MS directions coincident with the fixed beams in $\mathbf{U}_o$). The received SNR associated with each MS is given by $\rho n/K$ reflecting the $n$-fold array/beamforming gain of the AP antenna. The true sum capacity is achieved through dirty paper coding, which suffers from high complexity [19]. Our focus is on reduced-complexity linear precoders. For the general full-dimensional precoder in (10) we assess the conditional sum capacity for a given channel realization (random MS directions $\{\theta_k\}$) as

$$C(\rho, \mathbf{G}|\mathbf{H}) = \sum_{i=1}^{K} \log_2\left(1 + \mathrm{SINR}_i(\rho, \mathbf{G}|\mathbf{H})\right) \text{ bits/s/Hz} \quad (14)$$

where the interference is treated as noise and the signal-to-interference-and-noise (SINR) ratio for the $i^{\text{th}}$ user is

$$\mathrm{SINR}_i(\rho, \mathbf{G}|\mathbf{H}) = \frac{\rho\frac{|\alpha|^2}{K}|\mathbf{h}_i^H\mathbf{f}_i|^2}{\rho\frac{|\alpha|^2}{K}\sum_{m\neq i}|\mathbf{h}_m^H\mathbf{f}_i|^2 + \sigma^2} \ . \quad (15)$$

We can use the same relations for assessing the sum capacity of B-MIMO precoders as well by replacing $\mathbf{H}$ with $\mathbf{H}_b$ (full dimensional) and $\tilde{\mathbf{H}}_b$ (low dimensional), and $\mathbf{G}$ with $\mathbf{G}_b$ or $\tilde{\mathbf{G}}_b$. The ergodic sum capacity for a given precoder (determined by $\mathbf{G}$) is obtained as $C(\rho, \mathbf{G}) = E[C(\rho, \mathbf{G}|\mathbf{H})]$ where the averaging is over the random MS directions.

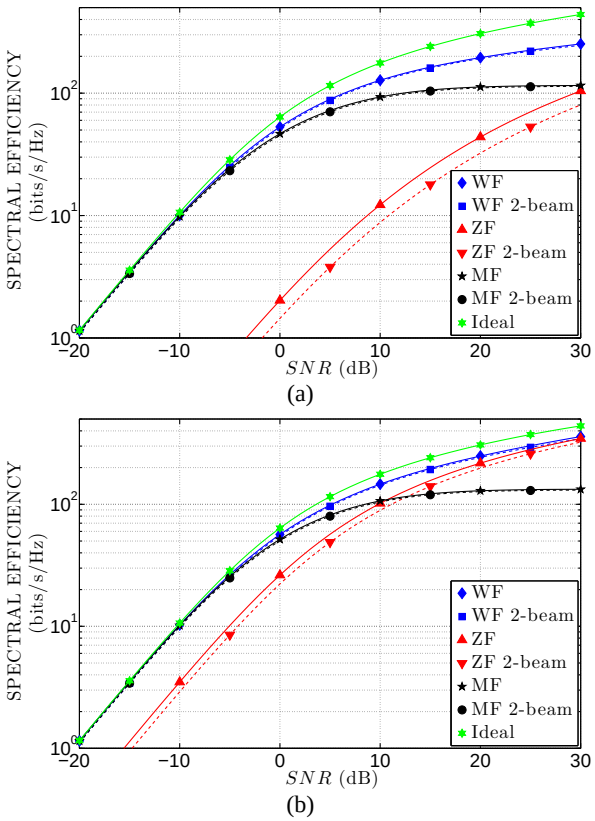


Fig. 3: (a) Capacity of three different B-MIMO precoders for downlink communication from an AP ($n = 81$) to $K = 40$ randomly distributed single-antenna MSs. (b) With minimum separation $\Delta\theta_{min} = \frac{\Delta\theta_o}{4}$.

Fig. 3 and Fig. 4 show numerical ergodic sum capacity results for the B-MIMO precoders generated by averaging over 2000 channel realizations for an AP equipped with a ULA of dimension $n = 81$ (linear 6" antenna at 80GHz) communicating with $K = 40$ or 60 single-antenna MSs over LoS links. The idealized upper bound is included for comparison. A 2-beam mask is used for complexity reduction, which from (9) captures at least 90 percent of the channel power on average ($E[\eta] \geq 0.9$). The MSs are randomly located over the entire spatial horizon ($-0.5 \leq \theta \leq 0.5$). The curves in Fig. 3(a) and Fig. 4(a) were generated with no restrictions on the MS LoS directions $\{\theta_k\}$ while the curves in Fig. 3(b) and Fig. 4(b) were generated with the a minimum MS LoS direction separation of $\Delta\theta_{min} = \frac{\Delta\theta_o}{4}$.

These plots show that the simplest MF precoder [19], [21], [22] performs well at lower SNRs due to the *approximate orthogonality* of high-dimensional user channels [8]. However there is always interference for finite $n$, resulting in performance loss at higher SNR. The ZF precoder completely eliminates interference, but significantly reduces the received signal power when the interference is high resulting in performance degradation (see Fig. 4(a)) [20]. The WF precoder achieves the best performance in all cases by adapting to the operating SNR (see (12)). Most importantly,

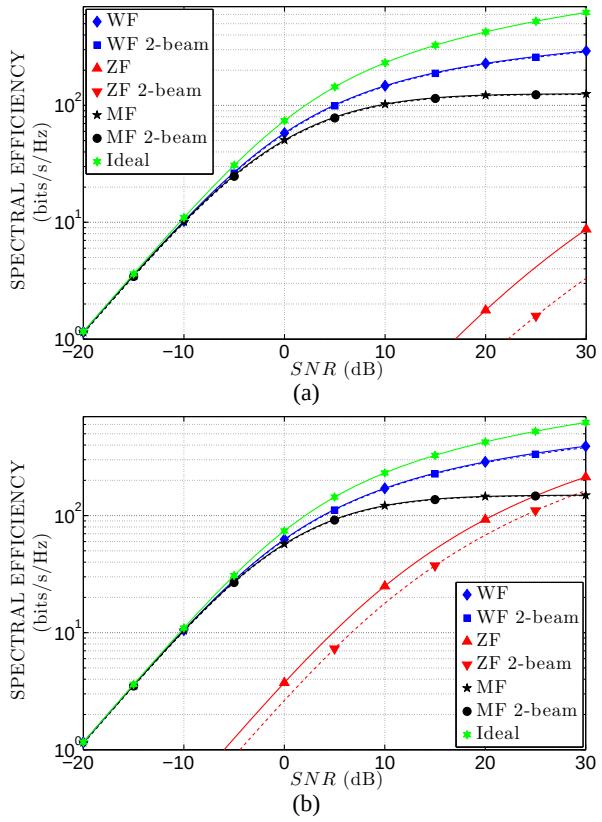


Fig. 4: (a) Capacity of three different B-MIMO precoders for downlink communication from an AP ($n = 81$) to $K = 60$ randomly distributed single-antenna MSs. (b) With minimum separation $\Delta\theta_{min} = \frac{\Delta\theta_o}{4}$.

the reduced-complexity B-MIMO precoders ($\tilde{\mathbf{G}}_b$) are able to closely approximate their full-dimensional counterparts ($\mathbf{G}_b$) except for the ZF precoder when the interference is high.

| | Spectral Efficiency (bits/s/Hz) | Aggregate rate (Gbps) | Average per-user rate (Gbps) |
|---|---|---|---|
| $K = 20$ $\Delta\theta_{min} = 0$ | 134 | 670 | 33.5 |
| $K = 20$ $\Delta\theta_{min} = \Delta\theta_o/4$ | 159 | 795 | 39.8 |
| $K = 40$ $\Delta\theta_{min} = 0$ | 192 | 960 | 24 |
| $K = 40$ $\Delta\theta_{min} = \Delta\theta_o/4$ | 243 | 1215 | 30.4 |
| $K = 60$ $\Delta\theta_{min} = 0$ | 226 | 1130 | 18.8 |
| $K = 60$ $\Delta\theta_{min} = \Delta\theta_o/4$ | 283 | 1415 | 23.6 |

TABLE I: Performance of the reduced-complexity B-MIMO WF precoders at an SNR of 20 dB with 5GHz of system bandwidth.

Table. I summarizes the performance of the reduced-complexity WF precoder when operating at an SNR of 20dB with 5GHz bandwidth for $K = 20$, 40, or 60 MSs and $\Delta\theta_{min} = 0$ or $\frac{\Delta\theta_o}{4}$. The table shows that enforcing a minimum user separation increases the data rate. However this comes at the cost of increased complexity. Fig. 5 plots $E[p]$ (average number of selected beams) for the 2-beam mask as a function of $K$. Clearly enforcing a minimum user separation requires the reduced-complexity precoders to select more beams on average. The maximum number of beams that the 2-beam mask can select (corresponding to the minimum complexity reduction) is $p_{max} = \min(2K, n)$. Fig. 5 shows that while for small $K$ $E[p] \approx p_{max}$, for larger $K$ $E[p]$ is generally smaller than $p_{max}$ with the largest gap when $K \approx \frac{n}{2}$.

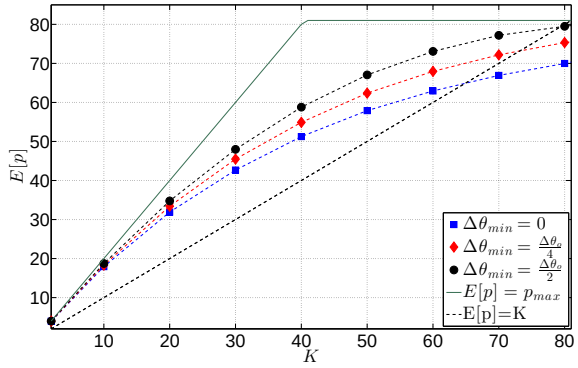


Fig. 5: $E[p]$ (average number of selected beams) using the 2-beam sparsity mask when $n = 81$.

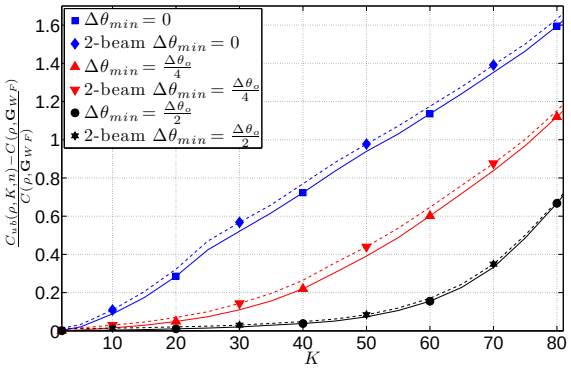


Fig. 6: Normalized capacity gap between the idealized upper bound and the WF precoder at an SNR of 30 dB

While the reduced-complexity WF precoder has the best performance, there is still residual interference between closely spaced MSs. This results in the idealized upper bound $C_{ub}$ overestimating the sum capacity achieved by the system. However, as shown in Fig. 6, when the interference is limited ($K \ll n$ and/or there is a minimum separation between the MSs) the approximation error between the true sum capacity for the WF precoders and $C_{ub}$ is minimal.

For an AP equipped with a uniform planar array of dimension $n = 6561$ (planar 6" $\times$ 6" antenna at 80GHz) communicating with $K = 100$ MSs over LoS links, $K \ll n$ so the interference will be low. Thus $C_{ub}$ provides an accurate estimate of the sum capacity of the WF precoder as 1268 bits/s/Hz. This corresponds to an average per-user rate of 63 Gbps with 5GHz bandwidth. If the AP is equipped with an analog beamforming front-end and uses a 4-beam mask for beam selection, the hardware complexity can be reduced an order-of-magnitude from 6561 to $p_{max} = 400$ RF chains.

## V. Conclusions

We have presented three precoders for high-dimensional MU-MIMO systems at mm-wave and higher frequencies that exploit the concept of B-MIMO for near-optimal complexity reduction. Optimal performance can be approached arbitrarily closely by increasing the number of selected beams (p). However, as our results demonstrate, beamspace channel sparsity at mm-wave enables near-optimal performance with transceiver complexity that tracks the number of MSs. At mm-wave the number of MSs is expected to be much lower than the system

dimension, enabling a significant reduction in DSP complexity as well as a reduction in hardware complexity in systems with analog beamforming front-ends. Thus, the combination of reduced-complexity B-MIMO precoders and analog beamforming provides a optimal trade-off between complexity and performance in mm-wave MU-MIMO networks.

## APPENDIX

In this appendix we bound the expected fraction of the channel power captured by the $m$-beam mask for the simple LoS channel model

$$E[\eta] = \frac{E[\mathrm{tr}(\tilde{\mathbf{H}}_b^H \tilde{\mathbf{H}}_b)]}{nK}. \quad (16)$$

Assuming that the $\{\theta_k\}$ are independently and identically uniformly distributed in $[-0.5,\ 0.5]$, $E[\eta]$ is equal to

$$\frac{1}{nK} E\left[\sum_{k=1}^{K}\sum_{i\in\mathcal{M}} |h_{b,k}(i)|^2\right] \geq \frac{1}{nK}\sum_{k=1}^{K} E\left[\sum_{i\in\mathcal{M}_k} |h_{b,k}(i)|^2\right] \quad (17)$$

where the inequality is due to the fact that $\mathcal{M}_k \subseteq \mathcal{M}$ and $|h_{b,k}(i)|^2 \geq 0$. Since the $\{\theta_k\}$ are i.i.d.

$$\frac{1}{nK}\sum_{k=1}^{K} E\left[\sum_{i\in\mathcal{M}_k} |h_{b,k}(i)|^2\right] = \frac{1}{n} E\left[\sum_{i\in\mathcal{M}_1} |h_{b,1}(i)|^2\right]. \quad (18)$$

For the $m$-beam mask, $\mathcal{M}_1$ selects the $m$ strongest elements of $\mathbf{h}_{b,1}$. The power of each element of $\mathbf{h}_{b,1}$ is

$$|h_{b,1}(i)|^2 = \left|\frac{\mathbf{a}_n^H(\theta_1)\mathbf{a}_n(i\Delta\theta_o)}{\sqrt{n}}\right|^2 = \frac{f_n^2(\delta + q(i,\ell)\Delta\theta_o)}{n} \quad (19)$$

where $\ell \in \mathcal{I}(n)$ is the index of the orthogonal beam closest to $\theta_1$, $\delta = \theta_1 - \ell\Delta\theta_o \in [-\frac{\Delta\theta_o}{2},\ \frac{\Delta\theta_o}{2}]$, $q(i,\ell) = \mathrm{mod}(\ell - i, \lfloor \frac{n}{2} \rfloor)$ is an integer representing the distance between the $\ell^{\mathrm{th}}$ and $i^{\mathrm{th}}$ orthogonal beams, and $f_n(\theta)$ is the Dirichlet sinc function [6], [7]. Arranging the elements of $\mathbf{h}_{b,1}$ according to decreasing power gives the following sequence for the $q(i,\ell)$

$$\mathcal{T} = \begin{cases} \{0, -1, 1, \ldots, c\} & \delta \geq 0 \\ \{0, 1, -1, \ldots, -c\} & \delta < 0 \end{cases} \quad (20)$$

where $c = \lfloor \frac{n}{2} \rfloor$ for odd $n$ and $c = -\frac{n}{2}$ for even $n$. Define $\mathcal{T}_m \subseteq \mathcal{T}$ as the set containing the first $m$ elements of $\mathcal{T}$. For the $m$-beam mask the $i \in \mathcal{M}_1$ correspond to the $q \in \mathcal{T}_m$, so the expectation in (18) is equal to

$$E\left[\sum_{q\in\mathcal{T}_m} \frac{1}{n} f_n^2(\delta + q\Delta\theta_o)\right]. \quad (21)$$

Calculating the expectation by integrating over the two cases of $\delta$, (21) is equal to

$$\int_{-\frac{\Delta\theta_o}{2}}^{0} \sum_{q\in\mathcal{T}_m} f_n^2(\delta + q\Delta\theta_o)d\delta + \int_{0}^{\frac{\Delta\theta_o}{2}} \sum_{q\in\mathcal{T}_m} f_n^2(\delta + q\Delta\theta_o)d\delta. \quad (22)$$

Since $f_n^2$ is an even function and $\mathcal{T}$ (also $\mathcal{T}_m$) is symmetric for the two cases of $\delta$, the final bound for $E[\eta]$ is

$$E[\eta] \geq \frac{2}{n}\int_{0}^{\frac{\Delta\theta_o}{2}} \sum_{q\in\mathcal{T}_m} f_n^2(\delta + q\Delta\theta_o)d\delta\ . \quad (23)$$

## REFERENCES


[1] V. Chandrasekhar, J. Andrews, and A. Gatherer, "Femtocell networks: a survey," *IEEE Commun. Mag.*, vol. 331, no. 6018, pp. 717–719, Sept. 2007.

[2] J. Andrews (moderator), "The Rapid Evolution of Cellular Networks: Femto, Pico and all that," in *Proc. 2011 Texas Wireless Summit (panel discussion)*, Oct. 2011.

[3] A. Goldsmith, *Wireless Communications*, Cambridge University Press, Cambridge, MA, 2006.

[4] I. E. Telatar, "Capacity of Multi-antenna Gaussian Channels," *Eur. Trans. on Telecommun.*, vol. 10, no. 6, pp. 585–595, Nov.-Dec. 1999.

[5] Z. Pi and F. Khan, "An Introduction to Millimeter-Wave Mobile Broadband Systems," *IEEE Commun. Mag.*, vol. 49, no. 6, pp. 101–107, June 2011.

[6] A. M. Sayeed and N. Behdad, "Continuous Aperture Phased MIMO: Basic Theory and Applications," in *Proc. Allerton Conf.*, Sept. 29-Oct. 1 2010, pp. 1196 –1203.

[7] A. M. Sayeed and N. Behdad, "Continuous Aperture Phased MIMO: A new architecture for optimum line-of-sight links," in *Antennas and Propagation, 2011 IEEE Int. Symp.*, July 2011, pp. 293 –296.

[8] T. L. Marzetta, "Noncooperative Cellular Wireless with Unlimited Numbers of Base Station Antennas," *IEEE Trans. Wireless Commun.*, vol. 9, no. 11, pp. 3590–3600, Nov. 2010.

[9] S. Sanayei and A. Nosratinia, "Antenna selection in MIMO systems," *IEEE Commun. Mag.*, vol. 42, no. 10, pp. 68–73, Oct. 2004.

[10] A. Mohammadi and F. Ghannouchi, "Single RF front-end MIMO transceivers," *IEEE Commun. Mag.*, vol. 49, no. 12, pp. 104–109, Dec. 2011.

[11] E. Torkildson, B. Ananthasubramaniam, U. Madhow, and M. Rodwell, "Millimeter-wave MIMO: Wireless links at optical speeds," in *Proc. Allerton Conf.*, Sept. 2006.

[12] C. Sheldon, M. Seo, E. Torkildson, M. Rodwell, and U. Madhow, "Four-channel spatial multiplexing over a millimeter-wave line-of-sight link," in *Proc. 2011 IEEE MTT-S Int. Microwave Symp.*, June 2009, pp. 389–392.

[13] F. Bohagen, P. Orten, and G. Oien, "Design of optimal high-rank line-of-sight MIMO channels," *IEEE Trans. Wireless Commun.*, vol. 6, no. 4, pp. 1420–1425, Apr. 2007.

[14] I. Sarris and R. Nix, "Maximum MIMO capacity in line-of-sight," in *2005 Int. Conf. on Information, Communications, and Signal Processing*, 2005, pp. 1236–1240.

[15] T. S. Rappaport, E. Ben-Dor, J. N. Murdock, and Y. Qiao, "38 GHz and 60 GHz Angle-dependent Propagation for Cellular & Peer-to-Peer Wireless Communications," in *IEEE Int. Conf. on Communications (ICC)*, June 2012.

[16] A. M. Sayeed, "Deconstructing Multiantenna Fading Channels," *IEEE Trans. Signal Processsing*, vol. 50, no. 10, pp. 2563–2579, Oct. 2002.

[17] J. Brady, N. Behdad, and A. Sayeed, "Beamspace MIMO for Millimeter-Wave Communications: System Architecture, Modeling, Analysis, and Measurements," *IEEE Trans. Antennas Propag.* to be published.

[18] V. Venkateswaran and A. van der Veen, "Analog Beamforming in MIMO Communications With Phase Shift Networks and Online Channel Estimation," *IEEE Trans. Signal Process.*, vol. 58, no. 8, pp. 4131–4143, Aug. 2010.

[19] D. Gesbert, M. Kountouris, R. Heath, C.B. Chae, and T. Salzer, "From single user to multiuser communications: Shifting the MIMO paradigm," *IEEE Signal Processing Mag.*, vol. 24, no. 5, pp. 36–46, Sep. 2007.

[20] M. Joham, W. Utschick, and J.A. Nossek, "Linear transmit processing in MIMO communications systems," *IEEE Trans. Signal Process.*, vol. 53, no. 8, pp. 2700–2712, Aug. 2005.

[21] A. Sayeed and T. Sivanadyan, "Wireless Communication and Sensing in Multipath Environments with Multi-antenna Wireless Transceivers," in *Handbook on Array Processing and Sensor Networks* 1st *ed.*, K. J. R. Liu and S. Haykin, Eds., pp. 115–170. IEEE-Wiley, Hoboken, NJ, 2010.

[22] T. Sivanadyan and A. Sayeed, "Space-time reversal techniques for wideband MIMO communication," in *Signals, Systems and Computers, 2008 42nd Asilomar Conf. on*, Oct 2008, pp. 2038–2042.